FRACTAL AND ITS STATISTICAL APPLICATIONS

KAITO NAKATANI

Abstract. Fractal is a popular geometry concept across many academic and practical areas: computer graphics, statistics, analysis, and artworks etc. Fractal also has many applications in analyzing data such as Brownian motion in chemistry, dynamical systems in chaos theory, and natural phenomena. This paper investigates a rigorous definition of fractal [8] and introduce some methods to analyze fractal data [3][8].

1. Introduction

A fractal is informally defined by a repeated appearance of similar shapes in a single object in different scales. This repeated appearance informally defines self-similarity. This informal definition of fractal includes both artificial and natural curves. A Blancmange (Takagi) Curve is a countinuous curve that is not differentiable everywhere, which is constructed by recursive midpoint subdivision [5]. Natural curves are often not as simple as geometric shapes such as circles, rectangles, or lines, so Mandelbrot approximates Britain's coastline using fractals in [6]. Another application of fractal appears in analyzing data that behaves like fractal such as web data or dynamical systems [8][9]. This paper is a literature investigation about fractal and its statistical applications. We assume that readers are CMSC 310 students and aim to introduce fractal to them. In this paper, we first introduce some examples of fractals (Section 2), introduce important definitions in discussing fractal such as the Hausdorff dimension (Section 3), fractal (Section 4), and similarity dimension (Section 5) with some concrete examples. Then, we show some applications of fractals in statistics (Section 6).

Date: May 10, 2019.

This document is a term paper for CMSC/Math 310 (Computational Geometry) at Bryn Mawr College.

2. Examples of Fractal

We begin by introducing some examples of fractal with figures. Notice that fractals introduced in this section might not be fractals under Definition 4.2, but we rather aim readers to have some concrete sense of what fractals look like. Fractals can be seen in many different occasions as following:

(1) Nature: Many natural phenomena such as the water amount of the Lake Albert [3, Section 8] or natural shapes such as snowflakes and the coast of Britain [7, Section 2] display self-similarity. Figure 1 shows leaves of fern with self-similarity. Notice that each branch of leaves are consisted of similar but smaller shapes, and this construction can be also seen in each branch as well.[1]

Figure 1. Self-similar shapes in leaves of fern.

(2) Mathematics: Many fractal curves display mathematically interesting properties such as Blancmange (Takagi) Curves as mentioned in Section 1.[2] Cantor sets display zero length and gives a further fractal curve called Devil's staircase by a process called curdling [3, Section 6]. Mathematical curves are also used to approximate fractal curves in nature; Kosh Curves are used to approximate snowflakes and the coast of Britain ultimately [7, Section 2]. Figure 2 shows an example of a Kosh Curve. This

[1]Figure 1 is taken from https://www.smithsonianmag.com/innovation/fractal-patterns-nature-and-art-are-aesthetically-pleasing-and-stress-reducing-180962738/.

[2]Blancmange Curves are not classified as fractals under Definition 4.2.

curve is constructed from a line segment by replacing the middle one-third with two line segments that form two edges of an equilateral triangle with the one-third length of the original line segment.[3]

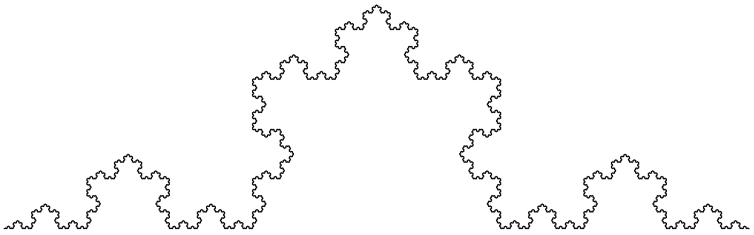

FIGURE 2. A Koch Curve.

(3) Artworks: Fractals can also be seen in many artworks. Leonardo Da Vinci's sketch of water flow shows a clear fractal structure, and imaginary landscapes called Gaussian hills are are applied in computer graphics [7, p.277]. Figure 3 is "The Great Wave off Kanagawa", the famous artwork in the 19th century from a Japanese print artist, Katsushika Hokusai [7, p. C16]. We can see fractal structures of the waves. [4]

FIGURE 3. Katsushika Hokusai's "The Great Wave off Kanagawa".

(4) Computational Geometry: We have seen some fractal shapes in our class as well. Figure 4 shows an example of fractals that we

[3]Figure 2 is taken from https://en.wikipedia.org/wiki/List_of_fractals_by_Hausdorff_dimension.
[4]Figure 3 is taken from https://www.youtube.com/watch?v=eoXoDOJrSpg.

have encountered in the class. We used this shape to consider a polygonal shape that achieves the maximum minimum number of vertex in a split polygon. We have also constructed a shape that achieves the worst-case for the number of the vertex guard by using a fractal construction. By its repetitive nature in different scales, fractal can often be used in arguing the worst-case scenario.

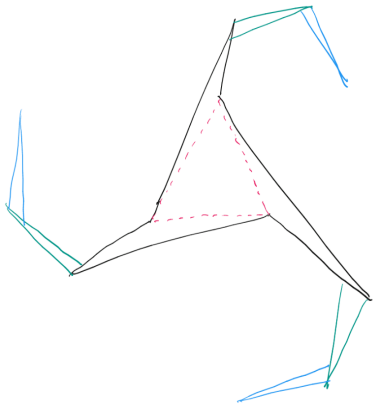

FIGURE 4. One of the possible answers for HW1 Question8(2).

3. The Hausdorff Dimension

While we have informally defined fractal, we define fractal more formally in Section 4. In order to define it, we first define the Hausdorff Dimension in this section and introduce some examples to calculate it.

Definition 3.1 ([8, p.32])**.** Let X be a set in $\mathbb{R}^m$ and $n(\epsilon)$ be the number of m-dimensional balls of diameter ϵ that are needed to cover X. If $n(\epsilon)$ increases like

$$n(\epsilon) \propto \epsilon^{-D} \quad \text{as} \quad \epsilon \to +0,$$

then D is the *Hausdorff Dimension* of X.

Note here that there are many ways to define fractal, but we use a method that uses the Hausdorff Dimension in this paper as other definitions often involve too many analytical and topological concepts that are beyond the scope of computational geometry course. Refer to [2, Chapter 2] for mathematical rigorous definition of the Hausdorff dimension that uses the Hausdorff Measure.

The Hausdorff Dimension intuitively defines how quickly the space is filling up more precisely than the topological dimension. We here introduce some examples to show how we calculate the Hausdorff Dimension of a shape.

Example 3.2. We calculate the Hausdorff Dimension of a closed line segment, $[0, l]$. Then, we can directly calculate

$$n(\epsilon) = \frac{l}{\epsilon} = l\epsilon^{-1} \propto \epsilon^{-1}.$$

Therefore, $D = 1$. □

Example 3.3. We calculate the Hausdorff Dimension of a Cantor Set. We construct C, a Cantor Set by taking a closed line segment $[0, 1]$ and removing the middle one-third of each line segment recursively. The set is as following:

$$C = [0,1] \setminus \left[\left(\frac{1}{3}, \frac{2}{3}\right) \cup \left(\frac{1}{9}, \frac{2}{9}\right) \cup \left(\frac{7}{9}, \frac{8}{9}\right) \cup \cdots \right].$$

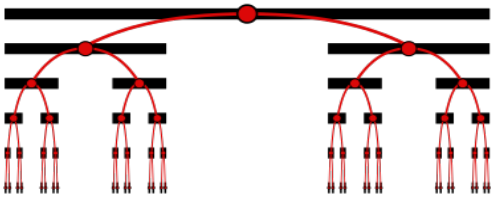

FIGURE 5. A Cantor Set.

Figure 5 shows the set C.[5] Each layer shows the result of removing the middle one-third of each line segment in the previous layer. We now calculate the Hausdorff Dimension. Notice that $n(\epsilon) = 1$ when $\epsilon \geq 1$. Assume that $n(\epsilon) = k$ when $\epsilon < 1$. Then, $n(\frac{\epsilon}{3}) = 2k$ because a line

[5]Figure 5 is taken from https://en.wikipedia.org/wiki/Cantor_set.

segment splits into two line segments that are scaled by $\frac{1}{3}$. Therefore,

$$\begin{aligned} & n\left(\frac{\epsilon}{3}\right) = 2n(\epsilon) \\ \Leftrightarrow & \left(\frac{\epsilon}{3}\right)^{-D} = 2\epsilon^{-D} \\ \Leftrightarrow & D = \frac{\ln 2}{\ln 3} \end{aligned}$$

□

4. Definitions of Fractals

Definition 3.1 enables us to state Proposition 4.1.

Proposition 4.1 ([6, p.15])**.** *Let X be a set in $\mathbb{R}^m$. If D is the Hausdorff dimension of X and D_T is the topological dimension of X, then $D \geq D_T$.*

Proposition 4.1 gives us a smooth introduction for Definition 4.2.

Definition 4.2 ([6, p.15])**.** Let X be a set in $\mathbb{R}^m$, D be the Hausdorff dimension of X, and D_T be the topological dimension of X. If $D > D_T$, then X is a *fractal* and D is the *fractal dimension* of X.

Recall that the Hausdorff Dimension records how quickly the space is filling up. Therefore, Definition 4.2 intuitively states that a fractal is filling up the space faster than its topological shape suggests.

Example 4.3. Example 3.2 shows that $D = 1$. Recall that $D_T = 1$ for the one-dimensional Euclidean space. Therefore, $D = D_T$, so it follows that a line segment is not a fractal.

Example 4.4. Example 3.3 shows that $D = \frac{\ln 2}{\ln 3}$. We know as an analytical fact that $D_T = 0$ for Cantor Sets. Therefore, $D > D_T$, so it follows that the set C is a fractal with the fractal dimension $\frac{\ln 2}{\ln 3}$.

5. Similarity Dimension

Some fractals are entirely self-similar, which means that they are invariant under scaling and translation. We now define the similarity dimension.

Definition 5.1 ([3, p.19])**.** Let S be a self-similar set. Suppose r be the scaling ratio and N be the number of nonoverlapping segments that need to cover the original set. Then,

$$D_S = -\frac{\ln N}{\ln r}$$

is the *similarity dimension*.

Theorem 5.2 ([3, p.19])**.** *If S is a self-similar fractral, then*

$$D = D_S.$$

Theorem 5.2 enables us to calculate the Hausdorff Dimension more easily.

Example 5.3. Consider the Cantor set. By inspection, it is a self-similar set. Note that the original set is scaled by $\frac{1}{3}$ and 2 scaled segments are needed to cover the original set. Therefore,

$$D_S = -\frac{\ln 2}{\ln \frac{1}{3}} = \frac{\ln 2}{\ln 3} = D.$$

6. Modeling Data

In this section, we introduce some examples where fractal is used in modeling data. While fractal analysis is an extremely broad and deep academic area, in order to fit in the range of 15 pages, we aim to introduce three examples, which are dynamical systems (Subsection 6.1), R/S analysis (Subsection 6.2), and Brownian Motion (Subsection 6.3), rather than going deep into one of them in this paper.

6.1. Dynamical Systems.

Dynamical system is a common topic in broad mathematics areas such as calculus, linear algebra, and chaos theory, and one of the most common methods in modeling data. We explore how modeling involves fractal in this subsection. This subsection is almost entirely based on [8, Section 1].

We first recall that the dynamical system is defined by the dynamical law,

$$x_{n+1} = f(x_n),$$

where x_n is the current state and x_{n+1} is the next state. We note here that not all dynamical systems are fractal.

Lemma 6.1 ([8, p.5, Modified])**.** *Let x_n be a state at time n with a dynamical low*

$$x_{n+1} = f(x_n, c)$$

where c is constant. If x displays a fractal structure, then the dynamical law is nonlinear.

Proof. Let $x_{n+1} = rx_n + c$ where r is a constant. Then, for $\alpha = \frac{c}{1-r}$, the following holds true:

$$x_{n+1} - \alpha = r(x_n - \alpha).$$

Then, if we let x_0 be the initial value,

$$x_n - \alpha = r^n(x_0 - \alpha) \Leftrightarrow x_n = \alpha + r^n(x_0 - \alpha),$$

which is an affine transformation of an exponential function. It follows that x does not display a fractal structure. □

We now illustrate an example that fractal model is used.

Example 6.2 ([8, Section 1]). Let x_n be the population size after n years after the year 0 with the population size $x_0 (\neq 0)$. Verhulst assumed the relative increase power, R, is proportional to $1 - x_n$ where 1 is the population size that is sustainable. This suggests that when the population size is bigger than 1, then the population size should decrease and when the population is smaller than 1, then the population size should increase. Then,

$$r(1 - x_n) = \frac{x_{n+1} - x_n}{x_n} (= R) \tag{6.1}$$

$$\Leftrightarrow \quad x_{n+1} = (1 + r)x_n - x_n^2, \tag{6.2}$$

where r is a positive constant. Therefore, the system is nonlinear dynamical system. We now find the fixed point of the system. Since we can find that $x_0 = 1$ stabilize the system at 1 by inspection, we assume that $x_n = 1$ is the stable point. Note here the first order Taylor approximation of Equation 6.2 at $x_n = 1$ is

$$x_{n+1} \approx (1 + r)(1) - r(1)^2 + \frac{(1 + r) - 2r(1)}{1!}(x_n - 1) \tag{6.3}$$

$$\Leftrightarrow x_{n+1} \approx 1 + (1 - r)(x_n - 1). \tag{6.4}$$

We now define $\delta_n = x_n - 1$, which denotes the deviation from 1. From Equation 6.4, we know that

$$\delta_{n+1} \approx (1 - r)\delta_n. \tag{6.5}$$

Therefore, when $0 < r < 2$, since $-1 < 1 - r < 1$, the system converges to 1. In a similar calculation, by using the dynamic law between x_{n+2} and x_n, we can obtain that if $r < \sqrt{6}$, then x_n oscillates periodically [8,

p.23].

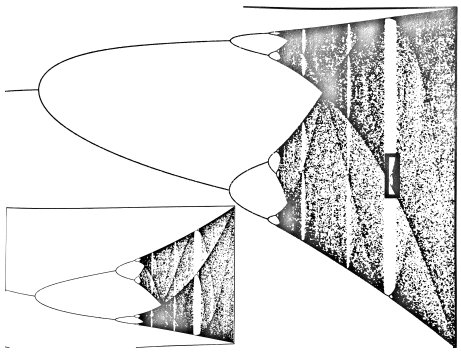

FIGURE 6. Verhulst population model. The horizontal axis is the r-axis and the vertical axis is the x-axis. The bottom-left part shows the detail of the black squared part.

Figure 6 is from [8, p.25] and shows the plot of 120 iterations of x after a transient period of 5000 iterations for each r in the range $(1.9, 3)$. We can see that at $r < 2$, there is only point that indicates the fixed point, $x = 1$, and at $r = 2$, the number of points increase to indicate the periodic oscillation. As r increases, the number of points further increases in the power of 2. This clearly shows a fractal structure, and is called Verhulst population model. The original paper further calculate the exact value of r where the tree splits in [8, p.25, 26] but we will not cover it in this paper.

Other examples of fractals that model different dynamical systems such as Julia Sets or the Mandelbolt Set can be seen in [8].

6.2. **R/S Analysis.** Rescaled range analysis (R/S analysis) was proposed by Hurst. His study yields some empirical results regarding how to analyze data over time that displays fractal structure. This subsection is almost entirely based on [3, Section 8, 11].

Data from natural phenomena often changes across time, and that becomes the point of interest of analysis: dependency between data and time. We first define several important terms to understand the set-up of R/S analysis.

Definition 6.3 ([3, Chapter. 8])**.** Let t be the time and γ be the time-span of an observation. If $Y(t)$ for $t = \{1, 2, \cdots, \gamma\}$ is the set of

observations at time t, then

$$\langle Y \rangle_\gamma = \frac{1}{\gamma} \sum_t Y(t),$$

$$X(t,\gamma) = \sum_{i=1}^{t} \{Y(i) - \langle Y \rangle_\gamma\},$$

$$R(\gamma) = \max_t X(t,\gamma) - \min_t X(t,\gamma), \quad \text{and}$$

$$S = \left(\frac{1}{\gamma} \sum_t \{Y(t) - \langle Y \rangle_\gamma\}^2 \right)^{\frac{1}{2}}.$$

Note here that intuitively $\langle Y \rangle_\gamma$ defines the mean of $Y(t)$ over the time period γ, $X(t,\gamma)$ defines the accumulated deviation from the mean at time t, $R(\gamma)$ defines the range of $X(t,\gamma)$, and S defines the standard deviation of $Y(t)$.

FIGURE 7. The Nikkei Index (the stock market index for Tokyo Stock Exchange) for one recent year until May 9th, 2019.

Example 6.4. We introduce a concrete example that explains Definition 6.3. Figure 7 shows the Nikkei Index for the past year.[6] While we do not calculate the Hausdorff dimension, the graph shows a fractal shape. Here,

$$t = \{1, 2, \cdots, 365\} \quad \text{and} \quad \gamma = 365.$$

[6]Figure 7 is taken from https://www.google.com/search?qnikkeistock&rlz1CAO TWH_enUS825& oqnikkeistack&aqschrome.1.69i57j0l5.3418j1j7&sourceidchrome&i eU TF8

Then, $\langle Y \rangle_\gamma$ is the mean price of the Nikkei index through out the year and $X(t, \gamma)$ is the accumulated difference from the mean up to time t. Therefore,

$$\langle Y \rangle_\gamma \approx 21940,$$
$$X(1, 365) \approx Y(1) - 21940 \approx 22497 - 21940 = 557,$$
$$X(2, 365) \approx Y(2) - 21940 + X(1, 365) \approx= 22758 - 21940 + 557 = 1375.$$

$R(\gamma)$ is the difference between the maximum index and the minimum index during the year, and S is the standard deviation. Then,

$$R(\gamma) = 24270 \text{ (Oct 2nd, 2018)} - 19156 \text{ (Dec 25th, 2018)} = 5114,$$
$$S = 1.4.^{7}$$

Example 6.4 shows one of the various applications of the set-up for the R/S analysis. The analysis can be used in all kinds of fractal data when the interest lies in the dependency of the time and the statistics. After investigating data from many natural phenomena such as the water amount of Lake Albert, sunspot numbers, or river discharges, Hurst proposed his empirical results as following:

Theorem 6.5 ([3, Chapter. 8])**.** *The rescaled range (R/S) of data is asymptotically proportional to*

$$R(\gamma)/S \approx \left(\frac{\gamma}{2}\right)^H$$

where H is the Hurst exponent.

Refer to [8, p.152] for various data that Hurst collected. While Feder provides with a very broad and deep arguments about R/S analysis using Theorem 6.5, we only see the overview of them. Theorem 6.5 gives us the following lemma that is useful in analyzing data.

Lemma 6.6 ([3, Chapter. 8])**.** *If the observation comes from i.i.d (identically distributed independent random variable), then*

$$R(\gamma)/S = \left(\frac{\pi\gamma}{2}\right)^{\frac{1}{2}}.$$

Feder shows that the simulation of tossing fair coins coincides with Lemma 6.6 both theoretically and practically [3, Chapter. 8.2]. Hurst also proposes that if H is significantly larger than $\frac{1}{2}$, then the data is persistent, and if H is significantly smaller than $\frac{1}{2}$, then the data

[7]This data is taken from https://www.macroaxis.com/invest/technicalIndicator/%5EN225–Standard-Deviation

is anti-persistent. However, Hurst recognizes that his measure is not really accurate and the memory effects of observations affect his data as well [3, Chapter. 8.3]. Feder extends his use of R/S analysis to wave-height statistics to discuss the effects of periodic elements in observations such as the influence of seasons on wave-height [3, Chapter. 11]. The applications of this analysis cover a broad area that involves non-Gaussian distribution or dependent variables, including Finance [1] and brain disorder [4].

We now connect the Hurst Exponent in R/S analysis with our knowledge about the fractal directly as following:

Theorem 6.7 ([3, Chapter. 10])**.** *Let X be a fractal data set. If H is the Hurst exponent of X and D is the fractal dimension of X, then*

$$D = 2 - H$$

holds locally.

In order to sketch the outline of the proof of Theorem 6.7, we need to discuss Brownian Motion first.

6.3. **Brownian Motion.** Brownian motion comes from a chemistry observation that describes small particles moving randomly. Random walk characterizes this motion, and randomness appears in various phenomena including biology, mathematics, and economics. This subsection introduces Feder's analysis of Brownian motion and is almost entirely based on [3, Section 9].
Brownian motion is characterized by its randomness. Therefore, Feder defines the random function as following:

Theorem 6.8 ([3, p.169])**.** *Let $X(t)$ be the position of a Brownian object at time t and the initial time be t_0. Then,*

$$X(t) - X(t_0) \approx \xi(t - t_0)^{\frac{1}{2}}$$

defines a random function of the object where ξ is a random value from the standard normal distribution.

Figure 8 shows the distribution of ξ and an example of $X(t)$ for a Brownian object where the horizontal axis denotes the time t.[8] We can generalize Theorem 6.8 by introducing the fractional Brownian motion. This takes the influence of memories into account i.e. the dependency between the previous state and the current state is considered.

[8]Figure 8 is taken from [8, p.165].

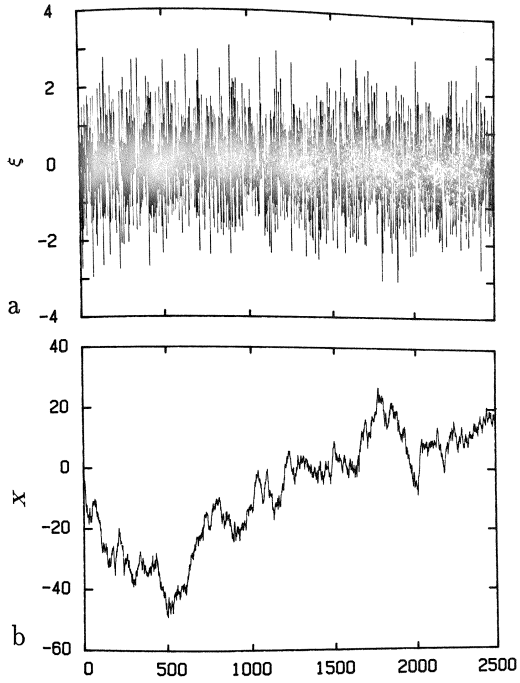

FIGURE 8. Independent random value from the standard normal distribution (above). The position X of a Brownian object at time t (below).

Theorem 6.9 ([3, p.172]). *Let $B_H(t)$ be the position of a Brownian object at time t. Then,*

$$B_H(t) - B_H(0) = \frac{1}{\Gamma(H+\frac{1}{2})} \int_{-\infty}^{t} K(t-t')dB(t')$$

where

$$K(t-t') = \begin{cases} (t-t')^{H-\frac{1}{2}}, & 0 \geq t' < t \\ (t-t')^{H-\frac{1}{2}} - (-t')^{H-\frac{1}{2}} & t' < 0 \end{cases}$$

defines a random function of the object where $dB(t')$ is previous increments for $t' < t$ of Gaussian random process.

Refer to [3, Chapter. 9] for the derivation of this formula. Notice that $H = \frac{1}{2}$ defines the memoryless random function since $\Gamma(1) = 0! = 1$. Feder also states that $H > \frac{1}{2}$ shows persistence and $H < \frac{1}{2}$ shows anti-persistence, similarly to the case of R/S analysis.

6.4. **Proof of Theorem 6.7.** In this subsection, we sketch the outline of the proof for Theorem 6.7. Refer to [3, Chapter. 10] for the complete argument. We first consider the trace of a fractal Brownian motion $B_H(t)$ of a Brownian object on a two-dimensional plane with time t on the horizontal axis and the position of the object on the vertical axis.

Proof. [3, p.186]

(1) Recall how we defined the Hausdorff Dimension in Section 3. Consider covering the original record using boxes with $b\gamma \times ba$ where $b \geq 1$. Similarly, let $N(b; a, \gamma)$ be the number of boxes needed to cover the whole trace of data. Then, there exists a unique D such that

$$N(b; a, \gamma) \sim b^{-D}.$$

(2) Notice that we divide time t into $b\gamma$ blocks. Then, for each $b\gamma$ segment, we need to cover $\Delta B_H(\gamma)$. We now consider Theorem 6.9 and obtain

$$B_H(b\gamma) - B_H(0) = \frac{1}{\Gamma(H + \frac{1}{2})} \int_{-\infty}^{b\gamma} K(b\gamma - t')dB(t').$$

By changing the variables by $t' = bt_a$, we obtain that $dB(t') = b^H dB(t_a)$ since $dB'(t)$ is a independent random process, and we further obtain $H = \frac{1}{2}$. Therefore,

$$B_H(b\gamma) - B_H(0) = \frac{1}{\Gamma(H + \frac{1}{2})} \int_{-\infty}^{t'} b^{\frac{1}{2}} K(b\gamma - bt_a)dB(t_a)$$

$$= \frac{1}{\Gamma(H + \frac{1}{2})} \int_{-\infty}^{t'} b^{\frac{1}{2}} (b)^{H-\frac{1}{2}} K(\gamma - t_a)dB(t_a) = b^H(B_H(\gamma)).$$

Then,

$$\Delta B_H(\gamma) = b^H(\Delta B_H(\gamma)).$$

(3) Since each block has the height ba, we need $\frac{b^H(\Delta B_H(\gamma))}{ba}$ boxes to cover each $b\gamma$ segment. Therefore,

$$N(b; a, \gamma) = \frac{b^H(\Delta B_H(\gamma))}{ba} \frac{T}{b\gamma} \approx b^{H-2}.$$

(4) We obtain that

$$b^{-D} \approx b^{H-2},$$

so $D = 2 - H$.

□

Notice that this results hold locally since we take $\gamma \ll T$ small. Feder shows that $D = 1$ globally. This shows the connection between our familiar fractal dimension of the fractal data and R/S analysis.

References

[1] A. Carbone, G. Castelli, and H.E. Stanley. "Time-dependent Hurst exponent in financial time series". In: *Physica A: Statistical Mechanics and its Applications* 344.1 (2004). Applications of Physics in Financial Analysis 4 (APFA4), pp. 267 –271. ISSN: 0378-4371. DOI: https://doi.org/10.1016/j.physa.2004.06.130. URL: http://www.sciencedirect.com/science/article/pii/S0378437104009471.

[2] Kenneth Falconer. *Fractal geometry*. Third. Mathematical foundations and applications. John Wiley & Sons, Ltd., Chichester, 2014, pp. xxx+368. ISBN: 978-1-119-94239-9.

[3] Jens. Feder. *Fractals*. eng. Physics of solids and liquids. New York: Plenum Press, c1988. ISBN: 0306428512.

[4] "Identifying major depressive disorder using Hurst exponent of resting-state brain networks". In: *Psychiatry Research: Neuroimaging* 214.3 (2013), pp. 306 –312. ISSN: 0925-4927. DOI: https://doi.org/10.1016/j.pscychresns.2013.09.008. URL: http://www.sciencedirect.com/science/article/pii/S0925492713002643.

[5] Jeffrey C. Lagarias. "The Takagi function and its properties". In: *Functions in number theory and their probabilistic aspects*. RIMS Kôkyûroku Bessatsu, B34. Res. Inst. Math. Sci. (RIMS), Kyoto, 2012, pp. 153–189.

[6] Benoit B. Mandelbrot. *Fractals: form, chance, and dimension*. Revised. Translated from the French. W. H. Freeman and Co., San Francisco, Calif., 1977, pp. xvi+365.

[7] Benoit B. Mandelbrot. *The fractal geometry of nature*. Schriftenreihe für den Referenten. [Series for the Referee]. W. H. Freeman and Co., San Francisco, Calif., 1982, pp. v+460. ISBN: 0-7167-1186-9.

[8] H.-O. Peitgen and P. H. Richter. *The beauty of fractals*. Images of complex dynamical systems. Springer-Verlag, Berlin, 1986, pp. xii+199. ISBN: 3-540-15851-0. DOI: 10.1007/978-3-642-61717-1. URL: https://doi.org/10.1007/978-3-642-61717-1.

[9] Shanyu Tang and Prof. Hassan Kazemian. "Simulation of Web Data Traffic Patterns Using Fractal Statistical Modelling". In: vol. 363. Jan. 2011, pp. 422–432. DOI: 10.1007/978-3-642-23957-1_47.